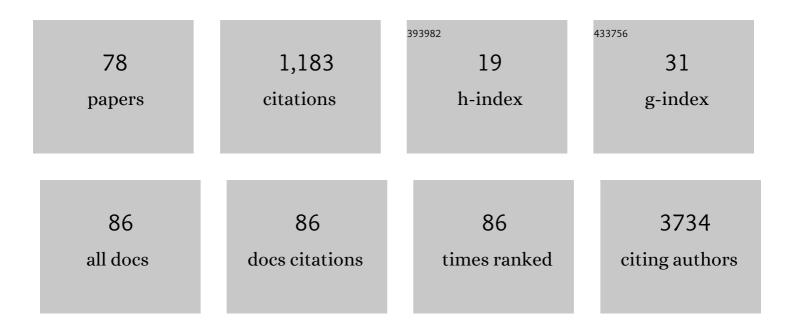


List of Publications by Year in descending order

Source: https://exaly.com/author-pdf/7440390/publications.pdf Version: 2024-02-01



#	Article	IF	CITATIONS
1	Fabrication of microfluidic channels with a circular cross section using spatiotemporally focused femtosecond laser pulses. Optics Letters, 2010, 35, 1106.	1.7	167
2	Direct fabrication of homogeneous microfluidic channels embedded in fused silica using a femtosecond laser. Optics Letters, 2010, 35, 282.	1.7	75
3	Femtosecond Laser Fabrication of Monolithically Integrated Microfluidic Sensors in Glass. Sensors, 2014, 14, 19402-19440.	2.1	70
4	Solar cycle, seasonal, and diurnal variations of subauroral ion drifts: Statistical results. Journal of Geophysical Research: Space Physics, 2014, 119, 5076-5086.	0.8	52
5	Two-photon fluorescence excitation with a microlens fabricated on the fused silica chip by femtosecond laser micromachining. Applied Physics Letters, 2010, 96, 041108.	1.5	44
6	Lenghu on the Tibetan Plateau as an astronomical observing site. Nature, 2021, 596, 353-356.	13.7	42
7	Fabrication of hollow optical waveguides in fused silica by three-dimensional femtosecond laser micromachining. Applied Physics B: Lasers and Optics, 2011, 105, 379-384.	1.1	39
8	Wide-field auroral imager onboard the Fengyun satellite. Light: Science and Applications, 2019, 8, 47.	7.7	35
9	Plasmapause surface wave oscillates the magnetosphere and diffuse aurora. Nature Communications, 2020, 11, 1668.	5.8	35
10	Doubleâ€peak subauroral ion drifts (DSAIDs). Geophysical Research Letters, 2016, 43, 5554-5562.	1.5	32
11	Tuning etch selectivity of fused silica irradiated by femtosecond laser pulses by controlling polarization of the writing pulses. Journal of Applied Physics, 2011, 109, .	1.1	27
12	A microfluidic chip integrated with a microoptical lens fabricated by femtosecond laser micromachining. Applied Physics A: Materials Science and Processing, 2011, 102, 179-183.	1.1	25
13	Moonâ€based EUV imaging of the Earth's Plasmasphere: Model simulations. Journal of Geophysical Research: Space Physics, 2013, 118, 7085-7103.	0.8	25
14	A new auroral boundary determination algorithm based on observations from TIMED/GUVI and DMSP/SSUSI. Journal of Geophysical Research: Space Physics, 2017, 122, 2162-2173.	0.8	25
15	A new solar windâ€driven global dynamic plasmapause model: 2. Model and validation. Journal of Geophysical Research: Space Physics, 2017, 122, 7172-7187.	0.8	24
16	Different Evolution Patterns of Subauroral Polarization Streams (SAPS) During Intense Storms and Quiet Time Substorms. Geophysical Research Letters, 2017, 44, 10,796.	1.5	24
17	Rapid fabrication of optical volume gratings in Foturan glass byÂfemtosecond laser micromachining. Applied Physics A: Materials Science and Processing, 2009, 97, 853-857.	1.1	22
18	Development and calibration of the Moon-based EUV camera for Chang'e-3. Research in Astronomy and Astrophysics, 2014, 14, 1654-1663.	0.7	19

#	Article	IF	CITATIONS
19	Data processing and initial results from the CE-3 Extreme Ultraviolet Camera. Research in Astronomy and Astrophysics, 2014, 14, 1664-1673.	0.7	19
20	Fabrication of three-dimensional microdisk resonators in calcium fluoride by femtosecond laser micromachining. Applied Physics A: Materials Science and Processing, 2014, 116, 2019-2023.	1.1	19
21	Determination of the Earth's plasmapause location from the CEâ€3 EUVC images. Journal of Geophysical Research: Space Physics, 2016, 121, 296-304.	0.8	18
22	Large‣cale Structure of Subauroral Polarization Streams During the Main Phase of a Severe Geomagnetic Storm. Journal of Geophysical Research: Space Physics, 2018, 123, 2964-2973.	0.8	18
23	Response of plasmaspheric configuration to substorms revealed by Chang'e 3. Scientific Reports, 2016, 6, 32362.	1.6	16
24	A new solar windâ€driven global dynamic plasmapause model: 1. Database and statistics. Journal of Geophysical Research: Space Physics, 2017, 122, 7153-7171.	0.8	16
25	Hemispheric asymmetry of subauroral ion drifts: Statistical results. Journal of Geophysical Research: Space Physics, 2015, 120, 4544-4554.	0.8	15
26	Inversion of the Earth's Plasmaspheric Density Distribution from EUV Images with Genetic Algorithm. Chinese Journal of Geophysics, 2012, 55, 1-9.	0.2	13
27	Analysis of observational data from Extreme Ultra-Violet Camera onboard Chang'E-3 mission. Astrophysics and Space Science, 2016, 361, 1.	0.5	13
28	Photoelectrons as a Tracer of Planetary Atmospheric Composition: Application to CO on Mars. Journal of Geophysical Research E: Planets, 2020, 125, e2020JE006441.	1.5	13
29	Search for squarks and gluinos in final states with one isolated lepton, jets, and missing transverse momentum at \$\$sqrt{s}=13\$\$ TeV with the ATLAS detector. European Physical Journal C, 2021, 81, 1.	1.4	13
30	Plasmaspheric trough evolution under different conditions of subauroral ion drift. Science China Technological Sciences, 2012, 55, 1287-1294.	2.0	12
31	Reconstruction of the plasmasphere from Moon-based EUV images. Journal of Geophysical Research, 2011, 116, n/a-n/a.	3.3	11
32	The Magnetospheric Driving Source of Doubleâ€Peak Subauroral Ion Drifts: Double Ring Current Pressure Peaks. Geophysical Research Letters, 2019, 46, 7079-7087.	1.5	11
33	Implantation of Earth's Atmospheric Ions Into the Nearside and Farside Lunar Soil: Implications to Geodynamo Evolution. Geophysical Research Letters, 2020, 47, e2019GL086208.	1.5	11
34	The solar wind plasma upstream of Mars observed by Tianwen-1: Comparison with Mars Express and MAVEN. Science China Earth Sciences, 2022, 65, 759-768.	2.3	10
35	Calculation of the extreme ultraviolet radiation of the earth's plasmasphere. Science China Technological Sciences, 2010, 53, 200-205.	2.0	9
36	Enhanced electron yield from laser-driven wakefield acceleration in high-Z gas jets. Review of Scientific Instruments, 2015, 86, 103502.	0.6	9

#	Article	IF	CITATIONS
37	Equatorial aurora: the aurora-like airglow in the negative magnetic anomaly. National Science Review, 2020, 7, 1606-1615.	4.6	9
38	Design and fabrication of far ultraviolet filters based on π-multilayer technology in high-k materials. Scientific Reports, 2015, 5, 8503.	1.6	8
39	On the Hardness of the Photoelectron Energy Spectrum Near Mars. Journal of Geophysical Research E: Planets, 2019, 124, 2745-2753.	1.5	8
40	Astrobiology at altitude in Earth's near space. Nature Astronomy, 2022, 6, 289-289.	4.2	8
41	Space solar telescope in soft X-ray and EUV band. Science in China Series G: Physics, Mechanics and Astronomy, 2009, 52, 1806-1809.	0.2	7
42	Onset of nonlinear self-focusing of femtosecond laser pulses in air: Conventional vs spatiotemporal focusing. Physical Review A, 2015, 92, .	1.0	7
43	Survival of the magnetotactic bacterium Magnetospirillum gryphiswaldense exposed to Earth's lower near space. Science Bulletin, 2022, 67, 1335-1339.	4.3	7
44	Configuration and performance of the ATLAS b-jet triggers in Run 2. European Physical Journal C, 2021, 81, 1.	1.4	7
45	EUV emissions from solar wind charge exchange in the Earth's magnetosheath: Threeâ€dimensional global hybrid simulation. Journal of Geophysical Research: Space Physics, 2015, 120, 138-156.	0.8	6
46	Evolution of the Subauroral Polarization Stream Oscillations During the Severe Geomagnetic Storm on 20 November 2003. Geophysical Research Letters, 2019, 46, 599-607.	1.5	6
47	Ancient Auroral Records Compiled From Korean Historical Books. Journal of Geophysical Research: Space Physics, 2021, 126, .	0.8	6
48	Hemispheric Asymmetry of the Vertical Ion Drifts at Dawn Observed by DMSP. Journal of Geophysical Research: Space Physics, 2018, 123, 10,213.	0.8	5
49	Tilt of the ring current during the main phases of intense geomagnetic storms. Science China Technological Sciences, 2019, 62, 820-828.	2.0	5
50	Equatorial auroral records reveal dynamics of the paleo-West Pacific geomagnetic anomaly. Proceedings of the National Academy of Sciences of the United States of America, 2021, 118, .	3.3	5
51	Statistical Characteristics of Giant Undulations During Geomagnetic Storms. Geophysical Research Letters, 2021, 48, e2021GL093098.	1.5	5
52	Correlations between plasmapause evolutions and auroral signatures during substorms observed by Chang'e-3 EUV Camera. Earth and Planetary Physics, 2017, 1, 35-43.	0.4	5
53	Thermal and stress studies of the 30.4nm Mo/Si multilayer mirror for the moon-based EUV camera. Applied Surface Science, 2014, 317, 902-907.	3.1	4
54	Statistical characteristics of the equatorial boundary of the nightside auroral particle precipitation. Science China Earth Sciences, 2015, 58, 1602-1608.	2.3	4

#	Article	IF	CITATIONS
55	The Magnetic Local Time Distribution of Storm Geomagnetic Field Disturbance Under Different Conditions of Solar Wind and Interplanetary Magnetic Field. Journal of Geophysical Research: Space Physics, 2019, 124, 2656-2667.	0.8	4
56	Development of a 3â€Ð Plasmapause Model With aÂBackâ€Propagation Neural Network. Space Weather, 2019, 17, 1689-1703.	1.3	4
57	A method to derive global O/N2 ratios from SSUSI/DMSP based on Re-AURIC algorithm. Journal of Atmospheric and Solar-Terrestrial Physics, 2020, 199, 105196.	0.6	4
58	Far-ultraviolet airglow remote sensing measurements on Feng Yun 3-D meteorological satellite. Atmospheric Measurement Techniques, 2022, 15, 1577-1586.	1.2	4
59	A Longâ€Term Data Set of Vertical Ion Drift Velocity at High Latitudes Constructed From DMSP Measurements. Journal of Geophysical Research: Space Physics, 2018, 123, 6090-6102.	0.8	3
60	Longitudinal dependence of ionospheric Poynting Flux in the Northern Hemisphere during quite times. Journal of Geophysical Research: Space Physics, 2021, 126, e2021JA029717.	0.8	3
61	Species-dependent solar rotation effects on the Martian ionosphere. Monthly Notices of the Royal Astronomical Society, 2022, 513, 1293-1299.	1.6	3
62	Remote sensing of planetary space environment. Chinese Science Bulletin, 2020, 65, 1305-1319.	0.4	2
63	THE OVERVIEW OF THE PLANETARY ATMOSPHERIC SPECTRAL TELESCOPE (PAST) IN THE SCIENTIFIC EXPERIMENTAL SYSTEM IN NEAR-SPACE (SENSE). International Archives of the Photogrammetry, Remote Sensing and Spatial Information Sciences - ISPRS Archives, 0, XLII-2/W13, 1419-1423.	0.2	2
64	Long-term variations in precipitable water vapor and temperature at Lenghu Site. Astronomy and Astrophysics, 2022, 663, A34.	2.1	2
65	High-Quality Laser-Driven Electron Beams by Ionization Injection in Low-Density Nitrogen Gas Jet. IEEE Transactions on Plasma Science, 2015, 43, 539-543.	0.6	1
66	Automatic Scheduling Tool for Balloon-Borne Planetary Optical Remote Sensing. Remote Sensing, 2021, 13, 1291.	1.8	1
67	Optical Remote Sensing of Planetary Space Environment. , 0, , .		1
68	The Frequencyâ€Domain Characterization of Cosmic Ray Intensity Variations Before Forbush Decreases Associated With Geomagnetic Storms. Space Weather, 2022, 20, .	1.3	1
69	Optomechanical design of a wide-field auroral imager on Fengyun-3D. Applied Optics, 2022, 61, 3349.	0.9	1
70	Correlations Between Giant Undulations and Plasmapause Configurations. Geophysical Research Letters, 2022, 49, .	1.5	1
71	Spatio-temporal manipulation of femtosecond pulses for 3D micro/nano-fabrication. , 2011, , .		0
72	In-situ and real time stress of 30.4 nm Mo/Si multilayer mirror for the moon-based EUV Camera. Proceedings of SPIE, 2014, , .	0.8	0

#	Article	IF	CITATIONS
73	Evolution of earth's plasmasphere in response to the solar wind variations and magnetic storms. , 2014, , .		0
74	High performance materials processing using tailored femtosecond laser pulses. , 2015, , .		0
75	Imaging of plasmasphere by Chang'e 3. , 2017, , .		0
76	On the structure of the Enceladus plume. Monthly Notices of the Royal Astronomical Society, 2021, 504, 6216-6222.	1.6	0
77	Evaluation of the 900‥ear European Auroral Records With Extreme Value Theory. Journal of Geophysical Research: Space Physics, 2021, 126, e2021JA029481.	0.8	Ο
78	Calibration of transition matrix of coordinate system for the aurora imager. Proceedings of SPIE, 2016, , .	0.8	0